Inorg. Chem. **2006**, *45*, 2199–2202

Theoretical Characterization of the "Very Rapid" Mo(V) Species Generated in the Oxidation of Xanthine Oxidase

Craig A. Bayse*

Department of Chemistry and Biochemistry, Old Dominion University, Hampton Boulevard, Norfolk, Virginia 23529

Received July 17, 2005

Density functional theory calculations of the "very rapid" Mo(V) intermediate of xanthine oxidase (XO) result in a square pyramidal geometry with end-on coordination of the model substrate. The Mo–C8 distance is 3.18 Å, longer than previously reported from ENDOR experiments (<2.4 Å Howes; et al. *Biochemistry* **1996**, *35*, 1432; 2.7–2.9 Å Mandikandan; et al. *J. Am. Chem. Soc.* **2001**, *123*, 2658). Theoretical gas-phase isotropic hyperfine coupling constants A_{iso}(C8) (B3LYP/BSII, 7.68 MHz; B3P86/BSII, 8.64 MHz) compare well with experimental values for the "very rapid" Mo(V) intermediate of XO with xanthine (8.8 MHz, Howes et al.) and 2-hydroxy-6-methylpurine (7.9 MHz, Mandikandan et al.). Absolute values of A_{iso} of the metal-bound substrate oxygen are similar in magnitude to that of experiment.

Introduction

Xanthine oxidase (XO) is the namesake of a family of molybdenum-containing enzymes which catalyze hydroxylation using water rather than O_2 as a source of oxygen atoms.[1] In the resting state, the square pyramidal coordination sphere of Mo consists of an axial oxo ligand, equatorial hydroxo and sulfido ligands, and the bidentate molybdopterin ligand (MPT). MPT is found in all monomolybdenum and -tungsten enzymes, and its role is to secure the metal to the protein, modulate the reduction potential, and shuttle electrons between distant redox centers. In the proposed mechanism of activity (Scheme 1),[1c] oxidation of xanthine occurs through simultaneous hydride transfer to the sulfido ligand and nucleophilic attack of activated hydroxo ligand upon the C8 carbon. Theoretical studies using formaldehyde and formamide as substrates confirm that this process is concerted and occurs through a tetrahedral arrangement around C8.[2] Oxidation of the Mo(IV) reduced state, **1** (Scheme 1), of the enzyme proceeds through two one-electron processes. An intermediate Mo(V) species, designated "very rapid" because of its short lifetime, has been detected by EPR, and characterization of its structure has been controversial.

Scheme 1

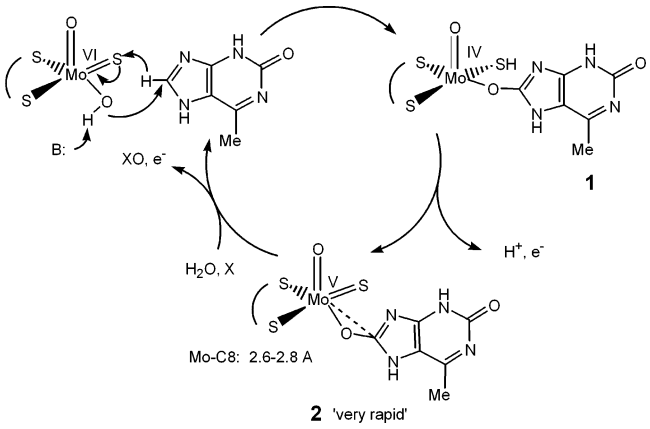

Early interpretation of electron−nuclear double resonance (ENDOR) experiments[3] claimed a direct Mo−C8 bond in analogy to η^2-acyl Mo(II) and Mo(IV) complexes on the basis of the Mo−C8 distance calculated from the expression for the anisotropic hyperfine coupling constant, T (eq 1). More recently, Manikandan et al.[4] reinterpreted the ENDOR data by decomposing T into local and nonlocal terms. Using only the nonlocal contribution and assuming exact sp^2 hybridization of C8, an Mo−C distance of 2.7−2.9 Å was

* To whom correspondence should be addressed. E-mail: cbayse@odu.edu.

(1) (a) Hille, R. *Chem Rev.* **1996**, *96*, 2757. (b) Hille, R. *Trends Biochem. Sci.* **2004**, *27*, 360. (c) Choi, E.-Y.; Stockert, A. L.; Leimkühler, S.; Hille, R. *J. Inorg. Biochem.* **2004**, *98*, 841. (d) Hille, R. *Arch. Biochem. Biophys.* **2005**, *433*, 107.

(2) (a) Ilich, P.; Hille, R. *J. Phys. Chem. B* **1999**, *103*, 5406. (b) Ilich, P.; Hille, R. *J. Am. Chem. Soc*. **2002**, *124*, 6796. (c) Zhang, X.-H.; Wu, Y.-D. *Inorg. Chem*. **2005**, *44*, 1466.

(3) Howes, B. D.; Bray, R. C.; Richards, R. L.; Turner, N. A.; Bennett, B.; Lowe, D. J. *Biochemistry* **1996**, *35*, 1432.

(4) Manikandan, P.; Choi, E.-Y.; Hille, R.; Hoffman, B. M. *J. Am. Chem. Soc*. **2001**, *123*, 2658.

10.1021/ic0511930 CCC: $33.50
Published on Web 02/08/2006

calculated. This length indicates end-on coordination to the metal.

$$T = \rho_{Mo} g_e \beta_e g_n \beta_n / r^3 \quad (1)$$

Theoretical studies of this enzyme have focused on the initial reductive half-reaction using small substrates such as formaldehyde or formamide.[2,5] In this article, the first calculations on the Mo(V) "very rapid" species are presented.

Theoretical Methods

Density functional calculations were performed using GAMESS-UK[6] using the B3LYP[7,8] and B3P86[7,9] exchange−correlation (XC) functionals and a relativistic effective core potential (RECP) basis set for molybdenum (5s5p4d)/[3s3s3d].[10] The Wadt−Hay ECP sulfur basis set[11] was augmented with s- ($\zeta = 0.036$) and p-type ($\zeta = 0.034$) diffuse functions for a final representation of (4s4p1d)/[3s3p1d]. Oxygen and C8 were represented by Dunning triple-ζ plus polarization functions basis sets.[12] Basis sets for hydrogen, nitrogen, and all other carbons were double-ζ quality.[13] Frequency calculations were used to verify that structures were minima on the potential energy surface.

Isotropic EPR hyperfine coupling constants, A_{iso}, for C8 and O_{Im} were calculated using eq 2 from the DFT optimized geometries using both BSI and alternate basis sets in which the Dunning TZVP basis sets are replaced with the IGLO-III[14] (C8) and EPR-II (C8, O_{Im}) and -III (C8, O_{Im}) basis sets.[15] Hybrid XC functionals are preferred for calculation of hyperfine coupling constants[16] because inclusion of HF exchange gives a better representation of the role of exchange in hyperfine splitting. A_{iso}(C8) was also calculated at the BSI geometries in a larger basis set (BSII) in which the metal basis set was uncontracted and augmented with f-type polarization functions ($\zeta = 0.7$) and diffuse d functions ($\zeta = 0.04$) (5221/5311/11111/1). In BSII, C8 was represented by EPR-III and diffuse functions ($\zeta_s = 0.085$; $\zeta_p = 0.055$) were added to oxygen.

$$A_{iso}(N) = \frac{4\pi}{3} \beta_e g_e \beta_N g_N \langle S_Z \rangle^{-1} \rho_N{}^{\alpha-\beta} \quad (2)$$

Results and Discussion

In the model of the XO active site (**1t** and **2t**), MPT was truncated to ethenedithiolate (EDT) and the xanthine substrate to imidazol (Im). The oxo ligand was arranged in the axial position and SH in the equatorial, consistent with results of magnetic circular dichroism studies of the "very rapid" intermediate.[17] According to the crystal structure of XO,[18] the phenyl rings of the Phe 914 and 1009 residues constrain the substrate to be planar with the axial oxo ligand.[19] The model system accounts for these environs by orienting Im such that a hydrogen-bonding interaction can exist between H_{Im} and the axial oxo group. A slightly lower-energy structure, **1tb** ($\Delta E \approx 2$ kcal/mol), can be found where H_{Im} hydrogen bonds to the sulfhydryl/sulfido ligand, but this orientation could not exist in the enzyme due to steric interference with the two Phe residues. The interaction between the oxo and H_{Im} may be unique to our small model system. Hydrogen bonding between oxo and Gln 767 and the xanthine substrate and either of the two glutamic acid residues above and below the Mo active site may dominate in the enzyme.

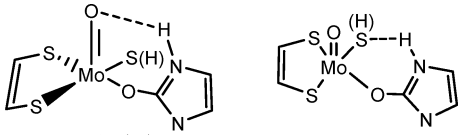

1t (H) **2t** **1tb** (H) **2tb**

The optimized geometry of **1t** shows a square pyramidal arrangement of ligands about the metal and Mo−OIm, Mo−SH, and Mo═O bond distances comparable to those reported by Voityuk et al.[5c] for the Mo(IV) formate species (2.16, 2.45, and 1.72 Å, respectively). Theoretical Mo−S and Mo−O distances for the EDT and oxo ligands are slightly longer than those found experimentally from EXAFS studies of reduced XO.[20] There is slight variation between the geometric parameters found with the two XC functionals. B3LYP gives longer Mo−S_{EDT} bond distances, and the Mo−C8 distance is shorter in B3P86.

Models of the "very rapid" Mo(V) species **2t** optimized to a square pyramidal configuration similar to **1t** with end-on coordination of the model substrate (Figure 1). To test for an η^2 interaction, calculations were also initiated from a structure with a short Mo−C8 distance. These models optimized to the end-on structure **2tb** which is ~2 kcal/mol

(5) (a) Voityuk, A. A.; Albert, K.; Köstlmeier, S.; Nasluzov, V. A.; Neyman, K. M.; Hof, P.; Huber, R.; Romão, M. J.; Rösch, N. *J. Am. Chem. Soc.* **1997**, *119*, 3159. (b) Bray, M. R.; Deeth, R. J. *J. Chem. Soc., Dalton Trans.* **1997**, 1267. (c) Voityuk, A. A.; Albert, K.; Romão, M. J.; Huber, R.; Rösch, N. *Inorg. Chem.* **1998**, *37*, 176.
(6) GAMESS-UK is a package of ab initio programs written by M. F. Guest, J. H. van Lenthe, J. Kendrick, K. Schoffel, and P. Sherwood with contributions from R. D. Amos, R. J. Buenker, H. J. J. van Dam, M. Dupuis, N. C. Handy, I. H. Hillier, P. J. Knowles, V. Bonacic-Koutecky, W. von Niessen, R. J. Harrison, A. P. Rendell, V. R. Saunders, A. J. Stone, D. J. Tozer, and A. H. de Vries. The package is derived from the original GAMESS code from Dupuis, M.; Spangler, D.; Wendoloski, J. *NRCC Software Catalog, Vol. 1, Program No. QG01 (GAMESS)*; 1980.
(7) Becke, A. D. *J. Chem. Phys.* **1993**, *98*, 5648.
(8) (a) Lee, C.; Yang, W.; Parr, R. G. *Phys. Rev.* **1988**, *B37*, 785. (b) Colle, R.; Salvetti, O. *Theor. Chim. Acta* **1975**, *37*, 329.
(9) Perdew, J. P. *Phys. Rev. B* **1986**, *33*, 8822.
(10) Lajohn, L. A.; Christiansen, P. A.; Ross, R. B.; Atashroo, T.; Ermler, W. C.; *J. Chem. Phys.* **1987**, *87*, 2812. (b) Couty, M.; Hall, M. B. *J. Comput. Chem.* **1996**, *17*, 1359.
(11) Wadt, W. R.; Hay P. J. *J. Chem. Phys.* **1985**, *82*, 284.
(12) Dunning, T. H. *J. Chem. Phys.* **1971**, *55*, 716.
(13) Dunning, T. H. *J. Chem. Phys.* **1970**, *53*, 2823.
(14) Kutzelnigg, W.; Fleischer, U.; Schlinder, M. in *NMR—Basic Principles and Progress*; Diehl, P., Fluck, E., Günther, H., Kosfeld, R., Eds.; Spirnger, Heidleberg, 1990; Vol. 23, p 165.
(15) Barone, V. In *Recent Advances in Density Functional Methods*, Part I; Chong, D. P., Ed.; World Scientific: Singapore, 1996.
(16) Hermosilla, L.; Calle, P.; Garcia de la Vega, J. M.; Sieiro, C. *J. Phys. Chem. A* **2005**, *109*, 1114 and references therein.
(17) Jones, R. M.; Inscore, F. E.; Hille, R.; Kirk, M. L. *Inorg. Chem.* **1999**, *38*, 4963.
(18) Enroth, C.; Eger, B. T.; Okamoto, K.; Nishino, T.; Pai, E. F. *Proc. Natl. Acad. Sci U.S.A.* **2000**, *97*, 10723.
(19) The author thanks an anonymous reviewer for pointing this out.
(20) Hille, R.; George, G. N.; Eidness, M. K.; Cramer, S. P. *Inorg. Chem.* **1989**, *28*, 4018.

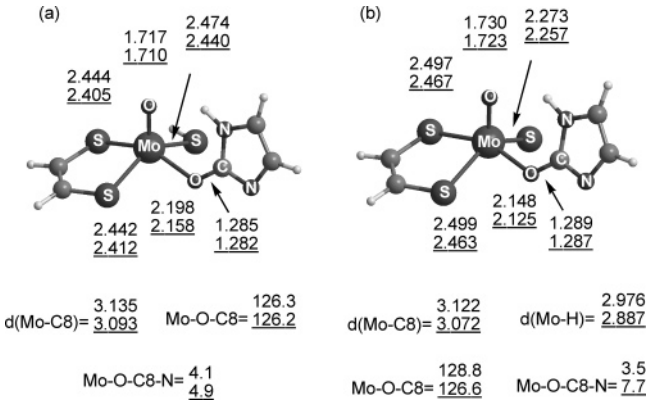

Figure 1. Selected structural parameters for (a) **1t** and (b) **2t** calculated at the B3LYP and B3P86 (underlined) levels. Distances are in Ångstroms; angles are in degrees.

Table 1. Mulliken Spin Populations and C8 Spin Density ($\rho^{\alpha-\beta}$) for **2t**

spin populations	B3LYP/BSI	B3P86/BSI
Mo	0.6809	0.6825
S	0.3586	0.3617
O_{oxo}	−0.0451	−0.0465
O_{Im}	0.0062	0.0049
C8	0.0001	0.0016
C_s	0.0017	0.0020
C_{px}	0.0004	0.0007
C_{py}	−0.0019	−0.0015
C_{pz}	−0.0002	0.0002
$\rho^{\alpha-\beta}_{C8}$	0.00676	0.00783

more stable than the structure forbidden by the Phe residues in the XO active site. The arrangement of the Im group allows for overlap between the C8 p_y atomic orbital (AO) and the singly occupied Mo d_{xy} orbital. The unpaired electron occupies the Mo d_{xy} orbital with significant delocalization onto the sulfido ligand according to Mulliken spin populations (Table 1).

Theoretical bond lengths and angles for **2t** (Figure 1b) are consistent with most parameters derived from experimental data. B3LYP and B3P86 Mo−oxo and Mo−OIm bond distances agree well with EXAFS data[21] for the oxidized Mo(VI) state of XO which also has a sulfido ligand. The DFT O−C8 bond lengths are ∼0.12 Å shorter than predicted from experiment (1.4 Å).[1d] The theoretical distance between Mo and the Im acidic proton (2.976 (B3LYP), 2.887 (B3P86), 3.030 Å) are shorter than results derived from electron spin−echo (ESEEM) studies[22] showing a single proton capable of exchange with solvent at 3.2 Å. The contentious Mo−C8 distance is longer than either of the values derived from ENDOR experiments, but given that the geometry optimization were initiated from structures where coordination was roughly η^2, it is clear that end-on coordination is preferred.

The short distance obtained with the qualitative method employed by Manikandan et al.[4] is likely due to the exact partitioning of the spin density into s and p contributions. Each atomic orbital was assumed to contribute equally to the spin density based upon the hybridization (see ref 4 for a full discussion). Mulliken spin populations (Table 1), however, show that most of the spin density is in the s- and p_y-type basis functions. Overweighting of the s AOs in the qualitative scheme led to an underestimation of the local contribution to the anisotropic hyperfine term and a smaller Mo−C8 bond distance. Mankandan et al. recognized the deficiencies of a qualitative scheme based upon hybridization and describe several more complicated corrections which would have increased the estimate of the Mo−C8 distance.

Table 2. Theoretical and Experimental Isotropic Hyperfine Coupling Constants A_{Iso} for **2t**

	exptl		BSI	BSIa[d]	BSIb[e]	BSIc[f]	BSII// BSI
A_{iso}(C8)	7.9,[a] 8.8[b]	B3LYP	7.82	7.92	7.76	7.51	7.68
		B3P86	8.81	8.95	8.75	8.45	8.64
$A_{iso}(O_{Im})$	37.8,[a] 34.2[c]	B3LYP	−33.60	−34.50		−34.30	
		B3P86	−35.72	−36.73		−36.16	

[a] Reference 3. [b] Reference 4, HMP = 2-hydroxy-6-methylpurine. [c] Reference 25, OMP = 2-oxo-6-methylpurine. [d] C8 or O_{Im} TZVP basis set replaced with EPR-II. [e] C8 or O_{Im} TZVP basis set replaced by IGLO-III. [f] C8 or O_{Im} TZVP basis set replaced by EPR-III.

Comparison of theoretically determined A_{iso} to experimental values has been used to evaluate theoretical structures for a variety of TM complexes of biological interest.[23] DFT calculations produce spin densities which incorporate electron correlation at lower cost with larger basis sets than possible for systems of biological interest with high-level ab initio methods. Previous studies have shown DFT A_{iso} values to be very dependent upon the chosen basis set and XC functional.[24] Hermosilla et al.[16] evaluated the quality of A_{iso} obtained from several XC functionals and commonly used basis sets in addition to the EPR-III basis set designed specifically for calculation of EPR data by improving the representation of the electron density in the core region.[15] The B3LYP functional was shown to give more reliable A_{iso} values than B3P86 or B3PW91. EPR-III and TZVP gave the best mean absolute deviations of the tested basis sets (3.02 and 4.66, respectively).[15]

Isotropic hyperfine coupling constants for C8 calculated from the optimized geometries of **2** agree well with experimental values (Table 2). A_{iso}(C8) at the B3LYP level was very close to the ENDOR data for HMP (7.9 MHz).[4] Values derived from B3P86 spin densities were in better agreement with experimental data for Xan (8.8 MHz).[3] Theoretical estimates of A_{iso}(C8) are smaller for the EPR-III modified basis set. Replacement of TZVP in BSI with the large EPR-III basis set might be considered too locally dense, so A_{iso}(C8) was also determined in a larger basis set (BSII) described in the Theoretical Methods section. These results did not significantly improve upon the BSI/EPR-III values. Differences between the theoretical model and experimental EPR data may be attributed to secondary

(21) Doonan, C. J.; Stockert, A.; Hille, R.; George, G. N. *J. Am. Chem. Soc.* **2005**, *127*, 4518.
(22) Lorigan, G. A.; Britt, R. D.; Kim, J. H.; Hille, R. *Biochim. Biophys. Acta* **1994**, *1185*, 284.
(23) (a) Neese, F. *Current. Op. Chem. Biol.* **2003**, *7*, 125 and references therein. (b) O'Malley, P. J.; Collins, S. J. *J. Am. Chem. Soc.* **2001**, *123*, 11042. (c) Schiemann, O.; Fritscher, J.; Kisseleva, N.; Sigurdsson, S. T.; Prisner, T. F. *ChemBioChem* **2003**, *4*, 1057.
(24) Munzarová, M. In *Calculation of NMR and EPR Parameters*; Kaupp, M., Bühl, M., Malkin, V. G., Eds.; Wiley-VCH: Weinheim, 2004; p 463.

interactions between Xan and HMP and the XO active site omitted from the theoretical model.

To provide further support for the structures in Figure 1, A_{iso} was also calculated for O_{lm}, which is more strongly coupled to the unpaired electron.[3] All XC functionals and basis sets give $A_{iso}(O_{lm})$ in good agreement with experimental data for Xan[3] and 2-oxo-6-methylpurine[25] "very rapid" Mo(V) states of the enzyme (Table 2). The spin difference is explained by the fact that only the magnitude of A_{iso} is determined in first-order EPR spectra.

Conclusions

While the above calculations cannot be used to definitively assign the structures in Figure 1 to the active site of the "very rapid" Mo(V) XO intermediate, they strongly suggest that its structure contains the substrate bonding to the metal in an end-on configuration with a bond distance of 3.1−3.2 Å. This distance confirms Manikandan et al.'s assignment and is consistent with other known examples of end-on coordination.[3] The discrepancies between experimental estimates of this distance show that complex decomposition schemes are necessary when interpreting hyperfine coupling data for centers with low spin density because contributions from the atom may be difficult to separate from nearby contributions. Computational studies bypass these schemes by directly calculating the spin density.

Acknowledgment. The author thanks an anonymous reviewer for many helpful suggestions.

Supporting Information Available: Cartesian coordinates and total energies for **1t** and **2t**. This material is available free of charge via the Internet at http://pubs.acs.org.

IC0511930

(25) Gutteridge, S.; Bray, R. C. *Biochem. J.* **1980**, *189*, 615.